MOX–Report No. 58/2013

Anisotropic adaptive meshes for brittle fractures: parameter sensitivity

Artina, M.; Fornasier, M.; Micheletti, S.; Perotto, S.

MOX, Dipartimento di Matematica "F. Brioschi"
Politecnico di Milano, Via Bonardi 9 - 20133 Milano (Italy)

mox@mate.polimi.it http://mox.polimi.it

Anisotropic adaptive meshes for brittle fractures: parameter sensitivity

Marco Artina[†], Massimo Fornasier[†], Stefano Micheletti[♯], Simona Perotto[♯]

November 20, 2013

[†] Faculty of Mathematics, Technische Universität München
Boltzmannstrasse 3, 85748, Garching, Germany
{marco.artina,massimo.fornasier}@ma.tum.de

[♯] MOX– Modellistica e Calcolo Scientifico
Dipartimento di Matematica "F. Brioschi", Politecnico di Milano
Piazza Leonardo da Vinci 32, I-20133 Milano, Italy
{simona.perotto,stefano.micheletti}@polimi.it

Keywords: non-convex minimization, brittle materials, a posteriori error estimators, anisotropic mesh adaptation

AMS Subject Classification: 65N30, 65N50, 74R10, 74G65, 65K10

Abstract

We deal with the Ambrosio-Tortorelli approximation of the well-known Mumford-Shah functional to model quasi-static crack propagation in brittle materials. We employ anisotropic mesh adaptation to efficiently capture the crack path. Aim of this work is to investigate the numerical sensitivity of the crack behavior to the parameters involved in both the physical model and in the adaptive procedure.

1 Introduction to the problem

The Mumford-Shah functional plays a key role in many applications, from image segmentation to mechanical problems [8]. One such application is the fracture propagation in brittle materials, where no predefined crack path is required. The Mumford-Shah functional is used for the first time by G. Francfort and J.-J. Marigo in [6] to model the quasi-static evolution of such a crack along the critical points of the energy. From a mathematical viewpoint, this leads to minimizing a nonconvex and nonsmooth functional which involves the displacement function u together with a lower dimensional set representing the crack Γ. This is an interesting challenge for both the theoretical analysis and the numerical computation.

In the two sections below we address a suitable regularization of the Francfort-Marigo functional and a corresponding discrete approximation. This smoothed model will allow us to tackle the numerical approximation via the employment of a suitable anisotropic adapted mesh, able to follow tightly the crack path.

1.1 The Modified Ambrosio-Tortorelli (MAT) functional

The functional provided by L. Ambrosio and V.M. Tortorelli is one of the most popular approach to dealing with the intrinsic irregularity of the Francfort-Marigo functional [1]. It is given by

$$I_\varepsilon(u,v) = \int_\Omega (v^2+\eta)|\nabla u|^2\, d\mathbf{x} + \kappa \int_\Omega \left[\frac{1}{4\varepsilon}(1-v)^2 + \varepsilon|\nabla v|^2\right] d\mathbf{x}, \tag{1}$$

where $\Omega \subset \mathbb{R}^2$ is an open domain, $0 < \eta \ll \varepsilon \ll 1$, $\kappa > 0$ approximates the elasticity constant of the material, while $u : H^1(\Omega) \to \mathbb{R}$ and $v : H^1(\Omega) \to [0,1]$ represent the displacement and the crack path, respectively. The first integral takes into account the elastic energy of the material, while the second integral is a fictitious energy spent in propagating the crack inside the material. Furthermore, when $v = 1$, the second integral vanishes, indicating the absence of a crack, whereas, when $v = 0$, only the fictitious energy does contribute and we are in the presence of an actual crack. The Ambrosio-Tortorelli functional enjoys the desirable property to Γ-converge to the Mumford-Shah functional [1].

To drive the crack evolution, an external load $g : \Omega \times [0,T] \to \mathbb{R}$ is applied on a subset $\Omega_{D^\pm}$ of Ω, defined as follows

$$g(\mathbf{x},t) = \begin{cases} \pm t & \text{if } \mathbf{x} \in \Omega_{D^\pm}, \\ 0 & \text{elsewhere}, \end{cases} \tag{2}$$

with $T > 0$ the final time of interest and $\mathbf{x} = (x_1, x_2)^T$. For simplicity, we denote hereafter $g(\mathbf{x},t)$ with $g(t)$. Let us also introduce the space of admissible solutions $\mathcal{A}(g(t)) = \{u \in H^1(\Omega) : u|_{\Omega_{D^\pm}} = g(t)|_{\Omega_{D^\pm}}\}$. Associated with the time interval $[0,T]$, we define a uniform partition $0 = t_0 < t_1 < \ldots < t_n = T$ of step Δt. According to a quasi-static evolution, at any time level t_k, with $k = 1, \ldots, n$, we solve the following minimization problem

$$(u_\varepsilon(t_k), v_\varepsilon(t_k)) \in \underset{\substack{u \in \mathcal{A}(g(t_k)), v \in H^1(\Omega) \\ \text{s.t. } v(\mathbf{x},t_k) = 0,\ \forall \mathbf{x} \in CR_{k-1}}}{\arg\min} I_\varepsilon(u,v), \tag{3}$$

with $CR_{k-1} = \{\mathbf{x} \in \overline{\Omega} \,|\, v_\varepsilon(t_{k-1}) < \texttt{CRTOL}\}$, and where `CRTOL` is a tolerance controlling somehow the thickness of the crack. At the initial time, we set $CR_{-1} = \emptyset$, i.e., the constraint in (3) is removed since the crack is not yet present. Convergence results relating the actual continuos model with the present time-discrete version can be found in [5].

In [2], we relax the constraints in (3) via suitable penalization terms which allow us to deal with an unconstrained minimization for the Modified Ambrosio-Tortorelli (MAT) functional

$$\begin{aligned} I_\varepsilon^{MAT}(u,v) &= \int_\Omega \left[(v^2+\eta)|\nabla u|^2\,d\mathbf{x} + \frac{1}{4\varepsilon}(1-v)^2 + \varepsilon|\nabla v|^2\right]\,d\mathbf{x} \\ &+ \frac{1}{\gamma_A}\int_{\Omega_{D^\pm}} (g(t_k)-u)^2\,d\mathbf{x} + \frac{1}{\gamma_B}\int_{CR_{k-1}} v^2\,d\mathbf{x}, \end{aligned} \tag{4}$$

where γ_A and γ_B are (small) penalty constants and $\kappa = 1$ is assumed for convenience. Moreover, as remarked in [2], condition $0 \le v \le 1$ is guaranteed by the minimization process.

1.2 The discretized MAT functional

We consider the discrete counterpart of the functional (4) via a finite element approximation. For this purpose, we introduce a family $\{\mathcal{T}_h\}$ of meshes of $\overline{\Omega}$ and denote by $\mathcal{E}_h$ the skeleton of $\mathcal{T}_h$. Moreover, we associate with $\mathcal{T}_h$ the space X_h consisting of continuous piecewise linear functions.

The discretization of the MAT functional based on X_h is

$$\begin{aligned} I_h^{MAT}(u_h,v_h) = &\int_\Omega \left[\left(P_h(v_h^2)+\eta\right)|\nabla u_h|^2\,d\mathbf{x} + \frac{1}{4\varepsilon}P_h((1-v_h)^2) + \varepsilon|\nabla v_h|^2\right]\,d\mathbf{x} \\ &+\frac{1}{\gamma_A}\int_{\Omega_{D^\pm}} P_h\left((g_h(t_k)-u_h)^2\right)\,d\mathbf{x} + \frac{1}{\gamma_B}\int_{CR_{k-1}} P_h\left(v_h^2\right)\,d\mathbf{x}, \end{aligned}$$

where $P_h : C^0(\overline{\Omega}) \to X_h$ is the Lagrangian interpolant onto X_h, and $g_h(t_k)$ is the $L^2(\Omega_{D^\pm})$-projection of $g(t_k)$ onto X_h. In practice, the minimization problem (3) is replaced by the following one

$$(u_h(t_k), v_h(t_k)) \in \underset{(\widehat{u}_h,\widehat{v}_h)\,\in\, X_h\times X_h}{\arg\min} I_h^{MAT}(\widehat{u}_h,\widehat{v}_h).$$

The critical points of I_h^{MAT} satisfy relation $(I_h^{MAT})'(u_h,v_h;\varphi_h,\psi_h) = 0$, where $(I_h^{MAT})'$ denotes the Fréchet derivative of the discrete MAT functional given, for any $(\varphi_h,\psi_h) \in X_h \times X_h$, by

$$\begin{aligned} &(I_h^{MAT})'(u_h,v_h;\varphi_h,\psi_h) \\ &= 2\left(\int_\Omega (P_h(v_h^2)+\eta)\nabla u_h\cdot\nabla\varphi_h\,d\mathbf{x} + \frac{1}{\gamma_A}\int_{\Omega_{D^\pm}} P_h\left((u_h-g_h(t_k))\varphi_h\right)\,d\mathbf{x}\right) \\ &+2\left(\int_\Omega \left[P_h(v_h\psi_h)|\nabla u_h|^2 + \frac{1}{4\varepsilon}P_h((v_h-1)\psi_h) + \varepsilon\nabla v_h\cdot\nabla\psi_h\right]\,d\mathbf{x}\right. \\ &\left.+\frac{1}{\gamma_B}\int_{CR_{k-1}} P_h\left(v_h\psi_h\right)\,d\mathbf{x}\right). \end{aligned}$$

The proof that the condition $0 \le v_h \le 1$ is automatically satisfied also in the discrete case can be found in [2].

2 The anisotropic a posteriori error estimator

We introduce now the basic setting useful to enrich the discretization above with mesh adaptation. In particular, we adopt an anisotropic approach due to the highly directional nature of the crack propagation as well as to the expected computational saving led by the employment of anisotropic meshes.
Following, e.g., [7], the geometric information describing a generic stretched element $K \in \mathcal{T}_h$ are the unit vectors $\mathbf{r}_{1,K}$ and $\mathbf{r}_{2,K}$ along the directions of the semi-axes of the ellipse circumscribed to K, and the positive scalars $\lambda_{1,K}$, $\lambda_{2,K}$, with $\lambda_{1,K} \geq \lambda_{2,K}$, which measure the length of these semi-axes. In practice, these quantities are computed by exploiting the spectral properties of the affine map T_K between the reference element $\widehat{K}$ and the actual triangle K, whose diameter and area are denoted by h_K and $|K|$, respectively.

The theoretical tool driving the adaptive procedure in Section 3 is provided by the following result, where we employ the standard notation $\|\cdot\|_{k,p,\varpi}$ to denote the norm in the Sobolev space $W^{k,p}(\varpi)$, with $\varpi \subset \mathbb{R}^d$ for $d = 1, 2$ and where k is omitted when zero.

Proposition 2.1 *Let $(u_h, v_h) \in X_h \times X_h$ be the critical point of I_h^{MAT}. Let us assume that $\#\Delta_K \leq \mathcal{N}$, where $\Delta_K = \{T \in \mathcal{T}_h : T \cap K \neq \emptyset\}$ is the patch of elements associated with K, and that $\mathrm{diam}(T_K^{-1}(\Delta_K)) \leq C_\Delta$. Then, for all $\varphi, \psi \in H^1(\Omega)$, there exists a constant $C = C(\mathcal{N}, C_\Delta)$ such that*

$$|(I_h^{MAT})'(u_h, v_h; \varphi, \psi)| \leq C \sum_{K \in \mathcal{T}_h} \left\{ \rho_K^A(v_h, u_h)\, \omega_K(\varphi) + \rho_K^B(u_h, v_h)\, \omega_K(\psi) \right\}, \quad (5)$$

where the residuals $\rho_K^A(\cdot,\cdot)$ and $\rho_K^B(\cdot,\cdot)$, and the weight $\omega_K(\cdot)$ are given by

$$\begin{aligned}
\rho_K^A(v_h, u_h) = {} & \|2 v_h \nabla v_h \cdot \nabla u_h\|_{2,K} + \tfrac{1}{2} \|[\![\nabla u_h]\!]\|_{\infty,\partial K} \|v_h^2 + \eta\|_{2,\partial K} \left(\frac{h_K}{\lambda_{1,K}\lambda_{2,K}} \right)^{\frac{1}{2}} \\
& + \frac{\delta_{K,\Omega_D^\pm}}{\gamma_A} \left(\|u_h - g_h(t_k)\|_{2,K} + \|g_h(t_k) - g(t_k)\|_{2,K} \right) \\
& + \frac{1}{\lambda_{2,K}} \left[\|v_h^2 - P_h(v_h^2)\|_{\infty,K} \|\nabla u_h\|_{2,K} + \frac{|K|^{1/2} h_K^2}{\gamma_A} |u_h - g_h(t_k)|_{1,\infty,K} \right], \\
\rho_K^B(u_h, v_h) = {} & \|(|\nabla u_h|^2 + \tfrac{1}{4\varepsilon}) v_h - \tfrac{1}{4\varepsilon}\|_{2,K} + \tfrac{\varepsilon}{2} \|[\![\nabla v_h]\!]\|_{2,\partial K} \left(\frac{h_K}{\lambda_{1,K}\lambda_{2,K}} \right)^{\frac{1}{2}} \\
& + \frac{\delta_{K,\mathrm{cr}_{k-1}}}{\gamma_B} \|v_h\|_{2,K} + \frac{h_K^2}{\lambda_{2,K}} \left[\| \, |\nabla u_h|^2 + \tfrac{1}{4\varepsilon} \|_{2,K} + \frac{|K|^{\frac{1}{2}}\, \delta_{K,\mathrm{cr}_{k-1}}}{\gamma_B} \right] |v_h|_{1,\infty,K}, \\
\omega_K(w) = {} & \left[\textstyle\sum_{i=1}^2 \lambda_{i,K}^2 (\mathbf{r}_{i,K}^T G_{\Delta_K}(w) \mathbf{r}_{i,K}) \right]^{1/2} \qquad \text{for } w = \varphi, \psi,
\end{aligned}$$

with $\delta_{K,\varpi}$ the Kronecker symbol associated with ϖ, such that $\delta_{K,\varpi} = 1$ if $K \cap \varpi \neq \emptyset$ and $\delta_{K,\varpi} = 0$ otherwise, $G_{\Delta_K} \in \mathbb{R}^{2\times 2}$ the symmetric matrix with entries $[G_{\Delta_K}(w)]_{i,j} = \int_{\Delta_K} \left(\partial w/\partial x_i\right) \left(\partial w/\partial x_j\right) d\mathbf{x}$, $i = 1, 2$, $[\![w_h]\!] = \left|[\partial w_h/\partial n]\right|$ on $\mathcal{E}_h \cap \Omega$ and $[\![w_h]\!] = \left|\partial w_h/\partial n\right|$ on $\mathcal{E}_h \cap \partial\Omega$ the jump of the normal derivative of $w_h = u_h, v_h$.

For the proof of this proposition, we refer to [2]. We just observe that an important role is played by the anisotropic estimates for the Clément quasi-interpolant [7]. The actual a posteriori error estimator, say η^{MAT}, involved in the adaptive procedure coincides with the right-hand side of (5) after replacing φ and ψ with u_h and v_h, respectively, and taking $C = 1$.

3 An optimize-and-adapt algorithm

The minimization of the functional I_h^{MAT} is a non-trivial task since it is non-convex. However, in [3] a first strategy to deal with it is proposed and further analyzed in [4]. The idea is to resort to a Gauss-Seidel-like algorithm consisting of a two-step procedure, first minimizing with respect to u_h for a fixed v_h, and then to minimize also with respect to v_h using the updated u_h. Moving from this idea, in [2] we couple this optimization step with an anisotropic mesh adaptation procedure in two different ways. In particular, following [7], we employ a metric-based approach relying on result (5) with the aim of minimizing the number of mesh elements for a fixed tolerance `REFTOL`$\ll 1$ on η^{MAT}. The first algorithm, optimize-then-adapt, in [2], which is a variant of `ALGORITHM 1` in [4], applies the mesh adaptation after convergence of the minimization algorithm on both u_h and v_h. Since the coupling between optimization and adaptation is not so tight, this algorithm is weak in the presence of sudden breakdowns of the material. As a consequence, in the second algorithm, optimize-and-adapt, we introduce a closer alternation of the optimization and mesh adaptation phases, by adapting the mesh just after two steps of the Gauss-Seidel algorithm without waiting for convergence.

In more detail, after fixing a termination tolerance `VTOL`$\ll 1$ for the minimization algorithm, a relative tolerance `MESHTOL`$\ll 1$ on the change of the mesh cardinality, the optimize-and-adapt algorithm is the following:

Optimize-and-Adapt Algorithm

1. Set $k = 0$, $\mathcal{T}_h^{(1)} = \mathcal{T}_h$;
2. If $k = 0$, set $v_h^1 = 1$; else $v_h^1 = v_h(t_{k-1})$;
3. Set $i = 1$; errmesh $= 1$; err$= 1$;

while errmesh $\geq$ `MESHTOL` & err $\geq$ `VTOL` **do**

4. $u_h^i = \arg\min_{z_h \in X_h^{(i)}} I_h^{MAT}(z_h, v_h^i)$;
5. $v_h^{i+1} = \arg\min_{z_h \in X_h^{(i)}} I_h^{MAT}(u_h^i, z_h)$;
6. Build the metric-based adapted mesh $\mathcal{T}_h^{(i+1)}$ with tolerance `REFTOL`;
7. err $= \|v_h^{i+1} - v_h^i\|_{\infty,\Omega}$;
8. errmesh $= |\#\mathcal{T}_h^{(i+1)} - \#\mathcal{T}_h^{(i)}|/\#\mathcal{T}_h^{(i)}$;
9. Set $v_h^1 = \Pi_{i \to i+1}(v_h^{i+1})$;
10. $i \leftarrow i + 1$;

end while

11. $u_h(t_k) = \Pi_{i-1 \to i}(u_h^{i-1})$; $v_h(t_k) = v_h^1$; $\mathcal{T}_h^k = \mathcal{T}_h^{(i)}$;

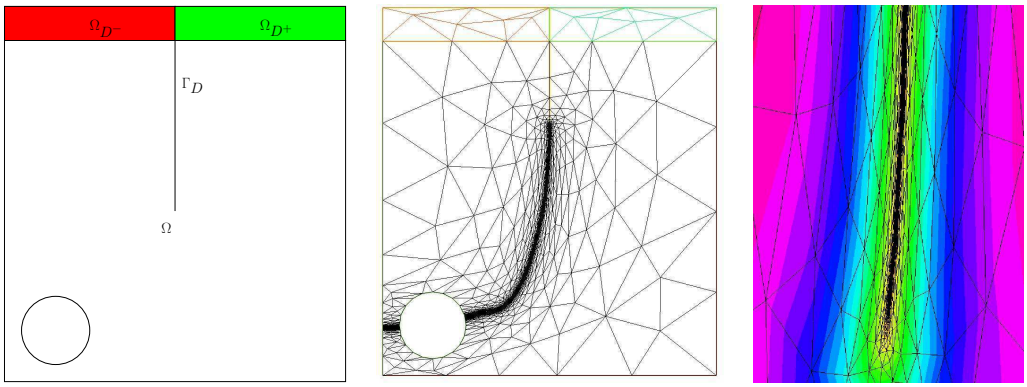

Figure 1: Computational domain (left), final anisotropic adapted mesh (center), zoom in (right) for the default parameters

12. Set $\mathcal{T}_h^{(1)} = \mathcal{T}_h^k$;
13. $k \leftarrow k + 1$;
14. if $k > n$, stop; else goto 2.

An interpolation step between two successive adapted meshes is employed before restarting any new optimization or time loop. This is carried out by a suitable interpolation operator, $\Pi_{j \to j+1}(w_h)$, which maps a finite element function w_h defined on $\mathcal{T}_h^j$ onto the new mesh $\mathcal{T}_h^{j+1}$. The convergence of the mesh adaptivity is checked by monitoring the change of the number of elements, which is an effective stopping criterion though not rigorously sound.

4 Sensitivity assessment

In this section we carry out a sensitivity analysis of the optimize-and-adapt algorithm to its main parameters. The test case used for this purpose is the curved crack configuration studied in [4, 2].
We consider a rectangle $\Omega = (0, 2) \times (0, 2.2)$ including the slit $\{1\} \times [1.5, 2.2]$, $2 \cdot 10^{-5}$ wide, and a circular hole of radius 0.2 and center at $(0.3, 0.3)$ (see Figure 1 (left)). In (2) we choose $\Omega_{D^-} = (0, 1) \times (2, 2.2)$ and $\Omega_{D^+} = (1, 2) \times (2, 2.2)$. The default values for the parameters are $\varepsilon = 2 \cdot 10^{-2}$, $\eta = 10^{-5}$, $\gamma_A = \gamma_B = 10^{-5}$, $\Delta t = 10^{-2}$, `CRTOL` $= 3 \cdot 10^{-4}$, `VTOL` $= 2 \cdot 10^{-3}$, `ADAPTOL` $= 10^{-2}$, and `REFTOL` $= 10^{-2}$. In Figure 1 we show the anisotropic mesh yielded by the algorithm at the final time $T = 1.43$ along with a detail around the crack. The number of the elements and the maximum aspect ratio $\max_{K \in \mathcal{T}_h} \lambda_{1,K}/\lambda_{2,K}$ are 15987 and $3.06 \cdot 10^3$, respectively. The first series of tests check on the sensitivity to the penalty constants $\gamma_A = \gamma_B$, by choosing three pairs of values, i.e., 10^{-4}, $5 \cdot 10^{-5}$, 10^{-5}. From Figure 2, it is evident that the higher the values of these constants, the larger is the deviation of the crack path with respect to the one assumed as

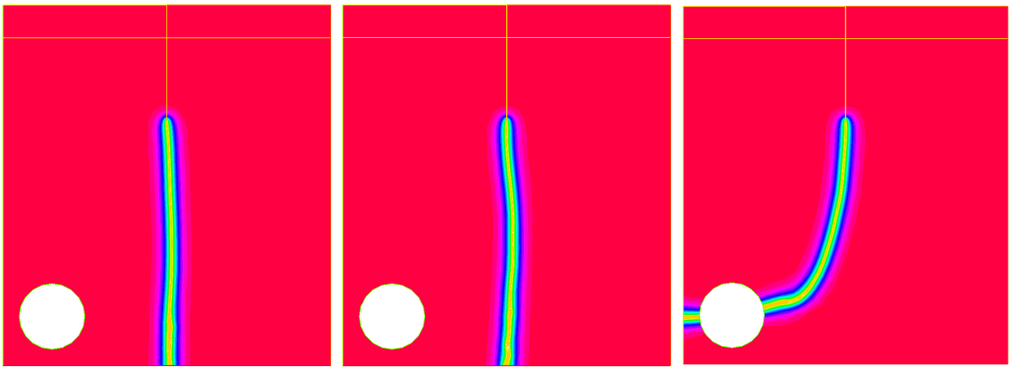

Figure 2: Sensitivity to the penalty constants: colour plot of the v_h-field for $\gamma_A = \gamma_B = 10^{-4}$ (left), $\gamma_A = \gamma_B = 5 \cdot 10^{-5}$ (center), $\gamma_A = \gamma_B = 10^{-5}$ (right)

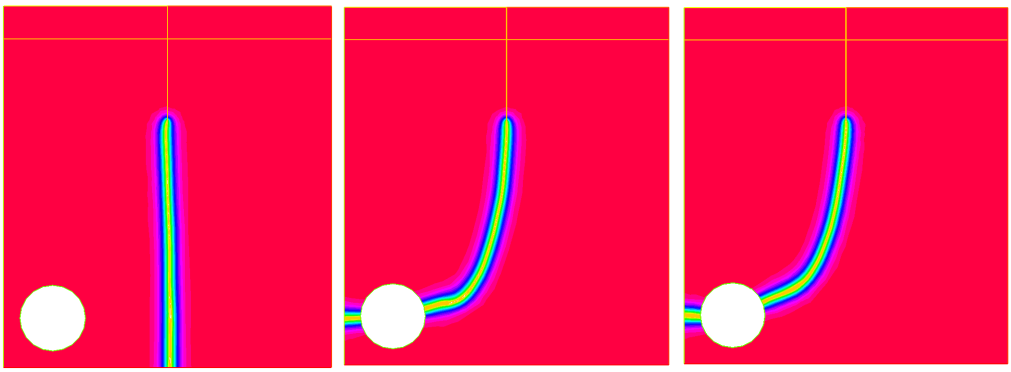

Figure 3: Sensitivity to `REFTOL`: colour plot of the v_h-field for `REFTOL`$= 10^{-1}$ (left), `REFTOL`$= 10^{-2}$ (center), `REFTOL`$= 8 \cdot 10^{-3}$ (right)

default. In particular, with the first two choices the crack even misses the hole. The two meshes yielding the straight path consist of fewer elements (12027 and 12628) than the default mesh in Figure 1.

The second trial of checks deals with the sensitivity to the tolerance `REFTOL` involved in the mesh adaptation procedure. We choose both a larger and a smaller value with respect to the default, namely `REFTOL`$= 10^{-1}$ and `REFTOL`$= 8 \cdot 10^{-3}$. The associated v_h-field are displayed in Figure 3. The largest value leads to a wrong path detection with only 8547 triangles, whereas the choice `REFTOL`$= 8 \cdot 10^{-3}$ identifies essentially the same path as the default one, but with an excessive number of elements (23521). Thus, it seems that too small a tolerance just increases the computational effort without improving the crack path tracking.

The last batch of tests assesses the behaviour of the optimize-and-adapt algorithm for a different value of ε, i.e., $\varepsilon = 5 \cdot 10^{-2}$. We observe that ε controls the

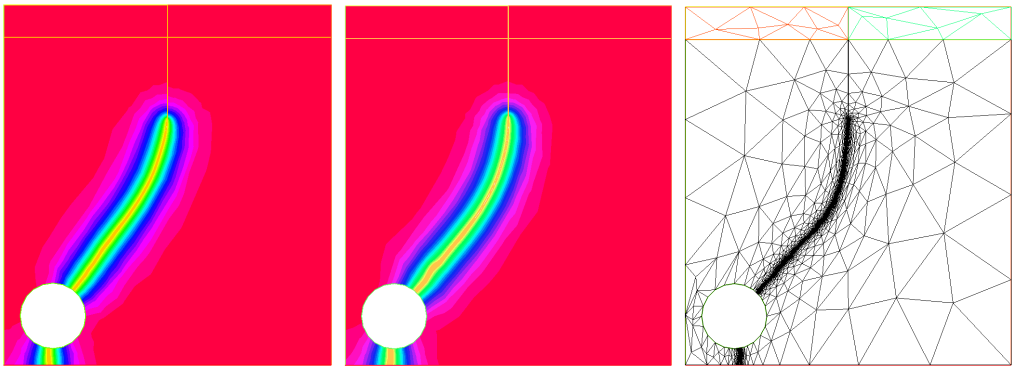

Figure 4: Colour plot of the v_h-field for REFTOL= 10^{-1} (left), REFTOL= 10^{-2} (center), and adapted mesh for $t = 1.43$ and REFTOL= 10^{-2} (right)

width of the crack. As expected, the larger value of ε widens the crack boundaries (compare the thickness of the crack in Figures 3 and 4). Moreover, also the crack trajectory changes considerably. For $\varepsilon = 5 \cdot 10^{-2}$ the crack suddenly turns left entering directly the hole, independently of the two chosen tolerances REFTOL= 10^{-1}, 10^{-2}. Although from a physical viewpoint the behavior seems correct, the bending of the actual path occurs too early and the crack leaves the hole downward instead to the left. A cross-comparison between Figures 3 and 4 leads to argue that for $\varepsilon = 5 \cdot 10^{-2}$ the value of REFTOL is not so crucial in identifying the actual path of the crack.

The assessment above seems to confirm that there is an actual sensitivity of the crack behaviour to the parameters involved in both the MAT functional and in the optimize-and-adapt algorithm. The employment of an anisotropic mesh adaptation seems strategical to explore the possible scenarios to single out the most reliable one, thanks to the computational saving due to an anisotropic grid.

References

[1] L. Ambrosio and V. M. Tortorelli, *Approximation of functional depending on jumps by elliptic functional via* Γ*-convergence*, Comm. Pure Appl. Math. **43**:8 (1990), 999–1036.

[2] M. Artina, M. Fornasier, S. Micheletti, and S. Perotto, *Anisotropic mesh adaptation for crack detection in brittle materials*, In preparation (2013).

[3] B. Bourdin, G. Francfort, and J.-J. Marigo, *Numerical experiments in revisited brittle fracture*, J. Mech. Phys. Solids **48**:4 (2000), 797 – 826.

[4] S. Burke, C. Ortner, and E. Süli, *An adaptive finite element approximation of a variational model of brittle fracture*, Society for Industrial and Applied Mathematics **48**:3 (2010), 980–1012.

[5] G. Dal Maso and R. Toader, *A model for the quasi-static growth of brittle fractures based on local minimization*, Math. Models Methods Appl. Sci. **12**:12 (2002), 1773–1799.

[6] G. Francfort and J.-J. Marigo, *Revisiting brittle fracture as an energy minimization problem*, J. Mech. Phys. Solids **46**:8 (1998), 1319 – 1342.

[7] S. Micheletti and S. Perotto, *Output functional control for nonlinear equations driven by anisotropic mesh adaption: the Navier-Stokes equations*, SIAM J. Sci. Comput. **30**:6 (2008), 2817–2854.

[8] D. Mumford and J. Shah, *Optimal approximations by piecewise smooth functions and associated variational problems*, Comm. Pure Appl. Math. **42**:5 (1989), 577–685.

MOX Technical Reports, last issues

Dipartimento di Matematica "F. Brioschi",
Politecnico di Milano, Via Bonardi 9 - 20133 Milano (Italy)

58/2013 Artina, M.; Fornasier, M.; Micheletti, S.; Perotto, S.
Anisotropic adaptive meshes for brittle fractures: parameter sensitivity

57/2013 Antonietti, P.F.; Perugia, I.; Zaliani, D.
Schwarz domain decomposition preconditioners for plane wave discontinuous Galerkin methods

56/2013 Antonietti, P.F.; Ayuso de Dios, B.; Mazzieri, I.; Quarteroni, A.
Stability analysis for Discontinuous Galerkin approximations of the elastodynamics problem

55/2013 Laadhari, A.; Ruiz-Baier, R.; Quarteroni, A.
Fully Eulerian finite element approximation of a fluid-structure interaction problem in cardiac cells

54/2013 Biasi, R.; Ieva, F.; Paganoni, A.M.; Tarabelloni, N.
Use of depth measure for multivariate functional data in disease prediction: an application to electrocardiographic signals

53/2013 Micheletti, S.
A continuum variational approach based on optimal control to adaptive moving mesh methods

51/2013 Chen, P.; Quarteroni, A.
Weighted reduced basis method for stochastic optimal control problems with elliptic PDE constraint

52/2013 Chen, P.; Quarteroni, A.; Rozza, G.
Multilevel and weighted reduced basis method for stochastic optimal control problems constrained by Stokes equations

47/2013 Chkifa, A.; Cohen, A.; Migliorati, G.; Nobile, F.; Tempone, R.
Discrete least squares polynomial approximation with random evaluations - application to parametric and stochastic elliptic PDEs

50/2013 Antonietti, P.F.; Verani, M.; Zikatanov, L.
A two-level method for Mimetic Finite Difference discretizations of elliptic problems